文章编号：1001-9014(2022)04-0702-08

DOI:10.11972/j.issn.1001-9014.2022.04.008

The effect of electron beam misalignment on confocal waveguide gyrotron traveling wave tube

YANG Jie[1,2*], XU Shou-Xi[1], WANG Yong[1,2], WANG Xiao-Yan[1,2]

(1. Key Laboratory of Science and Technology on High Power Microwave Sources and Technologies, Aerospace Information Research Institute, Chinese Academy of Sciences, Beijing 101400, China;
2. School of Electronic, Electrical and Communication Engineering, University of Chinese Academy of Sciences, Beijing 100049, China)

Abstract: In this paper, the effect of misaligned electron beam on the beam-wave interaction has been studied for a 0.22 THz confocal waveguide gyrotron traveling wave tube (gyro-TWT) with linear and nonlinear theory. The effect of electron beam misalignment on linear gain, critical current of absolutely instability and the exciting situation of backward wave oscillation is investigated by dispersion equation. A self-consistent nonlinear theory for confocal gyro-TWT is introduced to analyze the influence of electron beam misalignment on output power and beam-wave interaction efficiency. Meanwhile, the velocity spread is also taken into account to investigate the effect of electron beam quality on the confocal waveguide beam-wave interaction. The results show that the electron beam misalignments can cause efficiency degradation.

Key words: electron beam misalignment, confocal waveguide, terahertz, gyrotron traveling wave tube (Gyro-TWT)

PACS: 84.40.Ik

电子注偏心对共焦波导回旋行波管的影响

杨 杰[1,2*], 徐寿喜[1], 王 勇[1,2], 王笑妍[1,2]

(1. 中国科学院空天信息创新研究院 高功率微波源与技术国防科技创新重点实验室,北京 100140;
2. 中国科学院大学 电子电气与通信工程学院,北京 100049)

摘要:利用线性和非线性理论研究了电子注偏心对0.22 THz回旋行波管注波互作用的影响。基于色散方程研究了电子注偏心对线性增益、绝对不稳定性的起振电流和返波振荡的起振条件的影响。引入自洽非线性理论,分析了电子注偏心对输出功率和注波互作用效率的作用。同时,在考虑速度离散的情况下,研究了电子注质量对共焦波导注波互作用的影响。结果表明,电子注偏心会导致效率的降低。

关 键 词:电子注偏心;共焦波导;太赫兹;回旋行波管

文献标识码:A

Introduction

Terahertz (THz) science and technology is one of most prospective and essential academic fields, due to its high academic value and great application prospects, such as communications, radars, physics and materials science [1-3]. Gyro-TWT, based on convective instability, is the one of most promising THz sources, which can generate great power with broad gain bandwidth at the same time [4]. However, stability problem has always been a critical issue in the development of Gyro-TWTs. Heavily-load waveguide operated at fundamental or lower modes is one of the effective methods to control spurious oscillations [5]. Success has been achieved in gyro-TWT experiment at Ka-band with a ceramic loaded interaction structure and saturated peak power of 137 kW at 47 dB gain and 3-dB bandwidth of 1.11 GHz was obtained [6]. The demonstration of 140 kW of saturated out-

Received date: 2021-11-03, **revised date**: 2022-06-01 **收稿日期**:2021-11-03,**修回日期**:2022-06-01

Foundation items: Supported by National Natural Science Foundation of China (61571418, 61531002)

Biography: YANG Jie (1993-), female, Haerbin China, Ph. D. Research area involves novel high power microwave millimeter wave devices

* **Corresponding author**: E-mail: yangjie0334@163.com

put power, 28% of efficiency and 50 dB of gain at W-band by a gyro-TWT has been achieved [7].

The size of the interaction structure decreases with increase of frequency when gyro-TWT operates at the fundamental or lower modes. In order to ensure a large enough interaction structure to hold sufficient power, the gyro-TWT needs to operate in higher-order modes. However, working in higher-order modes would inevitably lead to serious mode competition [4,8]. Therefore, a stably working at high-order mode interaction structure, which can operate at high frequency with great power, is needed. Confocal waveguide, as an all-metal structure, which can not only suppress mode competition but also avoid the use of expensive and vulnerable lossy ceramic materials, is proposed and investigated [9]. R. J. Temkin applied the confocal structure to gyrotron at the first time [10], and MIT developed the theory and has successfully implemented confocal waveguide to gyro-TWT, which has achieved the power of 30 kW and 29 dB gain at 140 GHz.

However, the manufacture of gyro-TWT has the potential to bring about the electron beam misalignment and electron optical system plays an essential role in gyro-TWT [11]. Therefore, it is necessary to study the effect of electron beam misalignment on the performance of confocal gyro-TWT. The effect of parallel shifted electron beam on beam-wave interaction in gyrotron was investigated in linear theory in [12] and a nonlinear theory of gyrotron with the eccentricity of electron beam was developed in [13]. Meanwhile, the self-consistent time-dependent theory has been modified to analyze beam – wave interaction in gyrotron resonators in the case of a misaligned electron beam [14]. For its special field distribution, the traditional analyzing methods cannot be used directly to confocal waveguide in theoretical analyses [15]. To investigate the effect of misaligned electron beam on the linear gain, instabilities, power and efficiency, we extend those methods to the linear and nonlinear theory analyses of confocal waveguide gyro-TWT. This paper is organized as follows: Section 1 shows the features of confocal waveguide. Meanwhile, the coupling factor in confocal waveguide is also analyzed with the misaligned electron beam. Section 2 presents the results of effect of electron beam misalignment on the gain, absolute instability and backward wave oscillation (BWO) by solving the dispersion equation. Section 3 demonstrates a self-consistent nonlinear theory to analyze the beam-wave interaction with the misaligned electron beam and the effect of velocity spread on the efficiency is also considered. Finally, the summery is presented in Section 4.

1　Features of confocal waveguide

Confocal waveguide consists of two identical mirrors, separated by a distance $L_\perp$, equal to the radius of curvature of the mirrors R_c. For a 1D Gaussian mode TE_{0n} in the confocal waveguide, its membrane function can be presented as Ref. [4]:

$$\Psi_{0n}(x,y)=\begin{cases}\sqrt[4]{\dfrac{2}{\pi}}\sqrt{\dfrac{1}{w(y)}}\exp\left(-\dfrac{x^2}{w^2}\right)\cos\tau, n=2,4,6\cdots\\ \sqrt[4]{\dfrac{2}{\pi}}\sqrt{\dfrac{1}{w(y)}}\exp\left(-\dfrac{x^2}{w^2}\right)\sin\tau, n=1,3,5\cdots\end{cases}, \quad (1a)$$

$$w(y)=\sqrt{w_0^2+\frac{4y^2}{k_c^2w_0^2}}, \quad (1b)$$

$$\tau=-k_t\left(y+\frac{x^2}{2R}\right)+\frac{1}{2}\arctan\left(\frac{2y}{R_c}\right), \quad (1c)$$

$$R(y)=\frac{y^2+\left(k_tw_0^2/2\right)^2}{y}, \quad (1d)$$

where (x,y) is the coordination of electrons, and $w_0=\left(R_c/k_c\right)^{1/2}$ is the beam waist of wave, $R(y)$ is the phase front radius of curvature, $k_t=\pi(n+m/2+1/4)/R_c$ is the transverse wavenumber, and k_c is the cutoff wavenumber. We chose TE_{06} mode as the working mode to analyze a 0.22 THz confocal gyro-TWT.

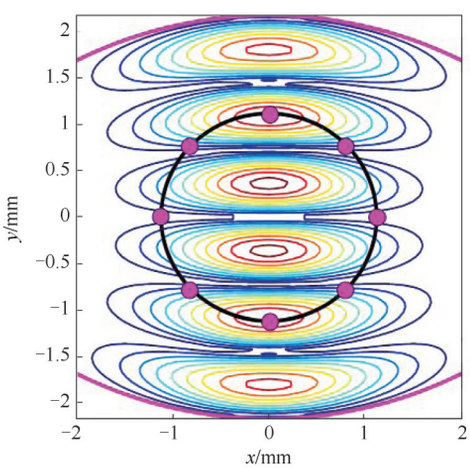

Fig. 1　Transversal electric field distribution of TE_{06} mode in the confocal waveguide overlaid with the distinct beamlets of annular electron beam

图 1　共焦波导中的 TE06 模式的横向电场分布和离散的环状电子注模型

With the local expansion of electron cyclotron orbit, we can rewrite $\Psi(x,y)$ as follows:

$$\Psi_{0n}(x,y)=\sum_{s=-\infty}^{\infty}J_s(k_cr_L)F_{0ns}(X,Y)e^{-js\phi}, \quad (2)$$

where $x=X+r_L\cos\phi$, $y=Y+r_L\sin\phi$, (X,Y) is the coordination of electron cyclotron center, r_L is the Larmor radius of electron, s is the harmonic number, J_s is the sth-order Bessel Function. The beam-wave coupling factor $F_{mns}(X,Y)$ which characterizes the Lorentz force of the high frequency field on the electron beam can be expressed as:

$$F_{0ns}(X,Y)=\left[\frac{1}{k_c}\left(\frac{\partial}{\partial X}+j\frac{\partial}{\partial Y}\right)\right]^s\Psi_{0n}(X,Y). \quad (3)$$

Figure 1 shows the schematic of TE_{06} mode and the annular electron beam which is discretized into distinct beamlets [17]. It is obvious that the value of coupling factor is related to the position of the guiding center due to the special structure of confocal waveguide. Therefore, the effect of the difference of the coupling factors at different guiding centers on the theoretical analyses must be taken into account. The optimal electron beam radius corresponding to TE_{06}mode can be determined as 1.12 mm in which case the beam is coupled with the second and fifth peaks along the y-axis. As shown in Fig. 2, when the harmonic numbers = 1, the value of $|F_{061}|^2$ is Gaussian distribution in the x-direction ($y = R_c/4$) and the six peaks of TE_{06}mode are evident along the y-axis direction. Figure 3 presents the variation of $|F_{061}|^2$ around the annular electron beam. It is easy to find that the beam-wave interaction is much stronger in the center of the mirrors (angle = $\pi/2$, $3\pi/2$) than that near the edge of mirrors (angle = 0, π), which is the reason for the asymmetric mode distribution of TE_{06} mode. For a confocal waveguide, a simple and effective way in theoretical analyses is to take the average of coupling factor as:

$$\left\langle |F_{0ns}|^2 \right\rangle = \frac{1}{P}\sum_{p=1}^{P} \left| (F_{0ns})_p \right|^2 \quad . \quad (4)$$

where P is the number of guiding centers. Figure 4 presents the cross section of cofocal waveguide with the misaligned elecreom beam and d is the misalignment distance. The variation of the interaction strength of working mode$TE_{06}$with the eccentricity distance can be derived from Eq. 4. As shown in Fig. 5, the coupling factor decreases with increase of eccentricity distance. The eccentricity has an influence on the performance of confocal gyro-TWT, so we will investigate the effect of eccentricity on the beam-wave interaction based on the linear and nonlinear theories.

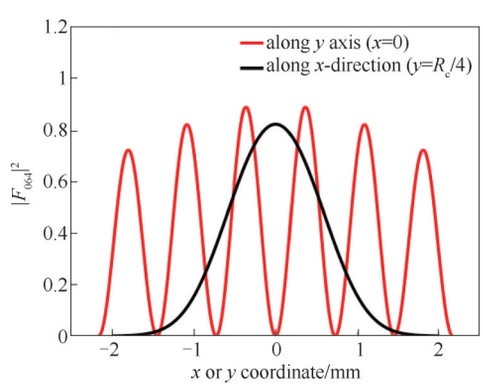

Fig. 2 Distribution of $|F_{061}|^2$ along a line $\left(y = R_c/4\right)$ in the x-direction and y-axis
图2 耦合系数沿着$y=R_c/4$和y轴方向的分布

2 Linear theory

In the view of electrodynamics theory, the linear dispersion equation derived from kinetic theory can be obtained by solving and transforming the Vlasov equation. Through the similar way in Ref. [18], making a special

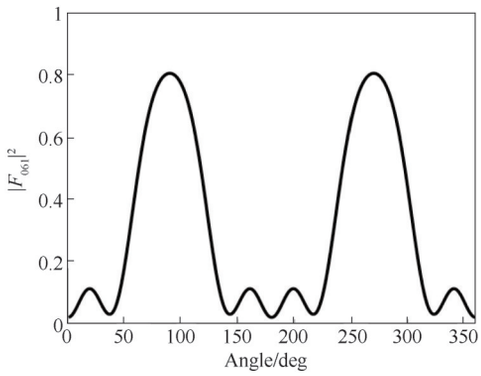

Fig. 3 Distribution of $|F_{061}|^2$ around the circle of R_b = 1.12 mm
图3 耦合系数在引导中心圆上的分布

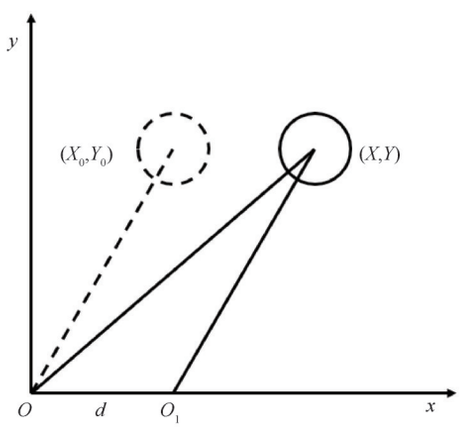

Fig. 4 Cross section of cofocal waveguide with the misaligned electron beam
图4 偏心电子注在共焦波导中位置图

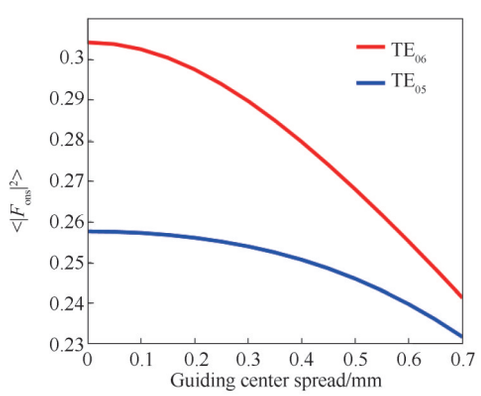

Fig. 5 The coupling factor with the increase of electron beam misalignment distance
图5 耦合系数随偏心距离的变化

deal with confocal waveguide field distribution, and neglecting the velocity spread and diffraction loss, the normalized linear dispersion equation for confocal waveguide can be expressed as:

$$D(\bar{k}_z,\bar{\omega}) = (\bar{\omega}^2 - \bar{k}_z^2 - 1)\left(\bar{\omega} - \beta_z \bar{k}_z - \frac{s\Omega_c}{\omega_c}\right)^2 = -\varepsilon = -\frac{I_b e \beta_t^2}{\gamma v_z \varepsilon_0 m_e k_c^2 c^2} \frac{\left\langle |F_{0ns}|^2 \right\rangle \left[J_s'(k_c r_L)\right]^2}{N_{0n}} \quad (5)$$

where $\bar{\omega} = \omega/\omega_c$ and $\bar{k}_z = k_z/k_c$ are the normalized frequency and axial wavenumber, respectively; $\omega_c = k_c c$, c is the light speed and $k_z = \sqrt{k^2 - k_t^2}$, $\beta_t = v_t/c$ and $\beta_z = v_z/c$ are normalized transverse and axial velocity, respectively; $\Omega_c = eB/\gamma m_e$, $\gamma = (1 - \beta_t^2 - \beta_z^2)^{-1/2}$, $r_L = \gamma m_e v_t/eB$ are the cyclotron frequency, relatively mass factor and Larmor radius of electron; e and m_e are electron charge and rest mass, respectively; B is the external magnetic field; ε is the dispersion parameter, I_b is the direct current of electron beam, and $N_{0n} = \iint_S \Psi_{0n}(x,y)\Psi_{0n}^*(x,y)\,\mathrm{d}S$.

Table 1　Operating parameters
表 1　工作参数

Parameter	Value
Frequency	0.22 THz
Mode	TE_{06}
Voltage /V	60 kV
Beam current/I_b	5 A
Velocity pitch factor/α	1.4
External magnetic field /B	8.17 T
Radii of curvature /R_c	4.35 mm
Mirror aperture/2a	4 mm
Radii of guiding center/R_b	1.12 mm

2.1　Linear gain

For a determinate operating frequency, the dispersion equation is a fourth-order polynomial of k_z. The linear growth rate can be defined by the imaginary part of forward growing wave. So the corresponding gain is described as:

$$\mathrm{Gain}(\mathrm{dB/cm}) = \frac{20}{\ln 10}|k_{zi}| \quad . \quad (6)$$

Figure 6 displays the effect of electron beam misalignment on the linear gain. When the operating parameters take the values in Table 1, it is obvious that the linear gain decreases with the increase of electron beam misalignment. Meanwhile, it is found that when the d increases, the linear gain will also decrease.

2.2　Absolute instability

The absolute instability in gyrotron was discussed in detail in Ref. [20]. The threshold condition of absolute instability is the saddle point of dispersion equation

$$D(\bar{k}_{zs},\bar{\omega}_{zs}) + \varepsilon = 0 \quad , \quad (7a)$$

$$\left.\frac{\partial D(\bar{k}_z,\bar{\omega})}{\partial \bar{k}_z}\right|_{(\bar{k}_{zs},\bar{\omega}_{zs})} = 0 \quad . \quad (7b)$$

When $B \approx B_g$ (B_g is the external magnetic field meets grazing condition), the critical current for absolute instability can be written as:

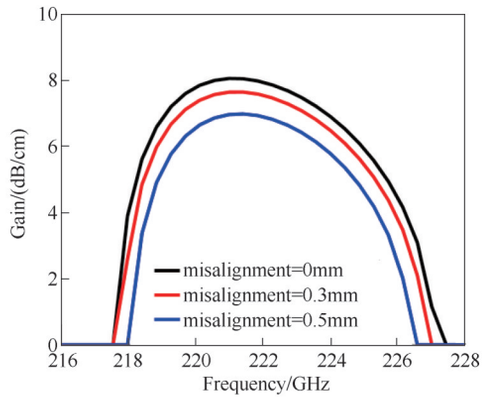

Fig. 6　Gain with different electron beam misalignment versus frequency
图 6　不同偏心距离时的增益

$$I_c = \frac{27\beta_z^2 \bar{k}_{zs}^4 k_{0n}^2 \varepsilon_0 m_e c^3}{e\beta_t^2} \frac{N_{0n}}{\left\langle |F_{0ns}|^2 \right\rangle \left[J_s'(k_c r_L)\right]^2} \quad , \quad (8)$$

where $\bar{\omega}_s = \left\{b_g + \left[8\beta_z^2(1 - b^2) + 64\beta_z^4\right]^{1/2}\right\} \Big/ (1 + 8\beta_z^2)$, $b_g = (1 - \beta_z^2)^{1/2}$ and $\bar{k}_{zs} = (\bar{\omega}_s - b_g)/4\beta_z$.

It can be concluded from the Fig. 7 that increasing the voltage can increase the critical current under the same magnetic field. According to the dispersion equation, as the voltage increases, the longitudinal velocity of the electron will increase, and the grazing point of the dispersion curve will move toward the high frequency direction. Therefore, an effective way to increase the critical current of absolute instability is to increase the voltage. It is also found that the critical current increases with the increase of the electron beam misalignment.

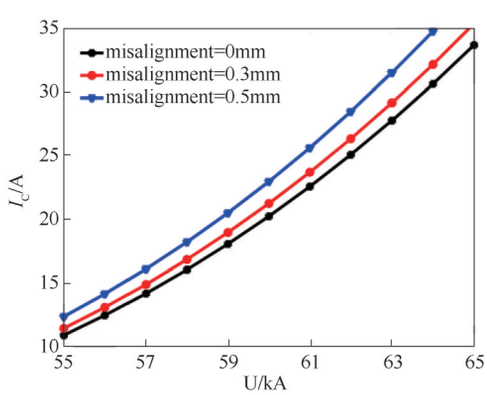

Fig. 7　Critical current of absolute instability versus voltage
图 7　绝对不稳定性起振电流随电压的变化

2.3　Backward wave oscillation

Based on the above analysis, the critical current of TE_{06} mode absolute instability can reach 20A, which is much higher than the operating current. Therefore, in the confocal waveguide Gyro-TWT design, the operating current usually does not depend on the critical current of absolute instability, but on the staring current of BWO. BWO is always a major factor of the stability of the Gyro-TWT. The starting current I_{st} of BWO can be derived as:

$$I_{st} = \frac{2\bar{\omega}_0 \beta_z^2 \bar{v}_g}{K_m}\left(\frac{\pi}{2L}\right)^3 \quad , \quad (9a)$$

$$K_m = \frac{-e\beta_t^2}{\gamma_0 \varepsilon_0 m_e c^3 \beta_z k_c^2}\frac{\left\langle \left| F_{0ns} \right|^2 \right\rangle}{N_{0n}^2}\left[J_s'\left(k_c r_L\right)\right]^2 . \quad (9b)$$

The main backward wave oscillation mode for the fundamentalTE$_{06}$ mode isTE$_{05}$ mode, which also has the smallest starting length of all the backward wave modes. Figure 8 illustrates the effect of electron beam misalignment on the starting current of BWO. When the operating current is 5 A and d is 0 mm, the critical interaction length ofTE$_{05}$ mode BWO is10.8 mm. It is found that the critical length of TE$_{05}$mode BWO increases from 10.8 to 11.2 mm when the electron beam misalignment d increases from 0 to 0.7 mm.

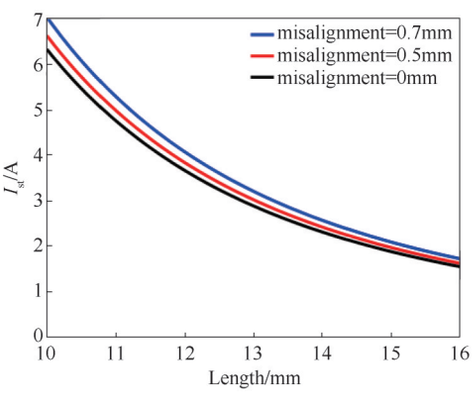

Fig. 8 Starting current of BWO versus length
图8 返波振荡的起振电流随长度的变化

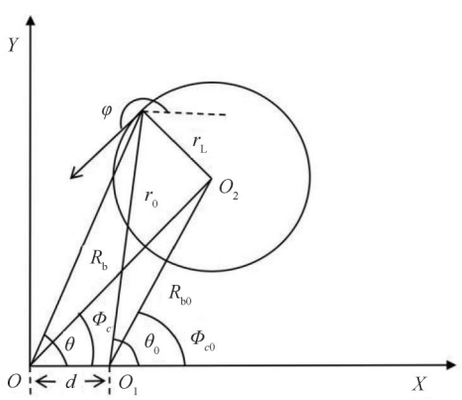

Fig. 9 Coordinate system for gyrating electrons with misalignment in a confocal waveguide
图9 共焦波导中回旋电子注偏心时的坐标系

3 Nonlinear theory

Figure 9 shows the cross section of a confocal gyro-TWT interaction structure and the coordinate parameters of electron beam with misalignment. $O(r,\theta,z)$is the center of the confocal waveguide and $O_1(r_0,\theta_0,z)$ is the center of misaligned annular electron beam; d is the distance between two centers. The parameters in coordinate system O can be expressed as:

$$R_b = \sqrt{R_{b0}^2 + d^2 - 2R_{b0}d\cos\phi_{c0}} \quad , \quad (10a)$$

$$\phi_c = \arctan\left(\frac{R_{b0}\sin\phi_{c0}}{R_{b0}\cos\phi_{c0} + d}\right) \quad , \quad (10b)$$

$$r = \sqrt{R_b^2 + r_L^2 + 2R_b r_L \sin(\varphi - \phi_c)} \quad , \quad (10c)$$

$$\theta = \arctan\left(\frac{-r_L\cos(\varphi - \phi_c)}{R_b - r_L\sin(\varphi - \phi_c)}\right) \quad . \quad (10d)$$

By neglecting the beam effects on the transverse field distribution, fields of TE$_{0n}$mode in a confocal waveguide gyro-TWT can be demonstrated as follows:

$$\begin{cases} H_z(x,y,z) = f(z)\Psi_{0n}(x,y)e^{j\omega t} \\ H_x(x,y,z) = -\dfrac{jk_z f(z)}{k_c^2}\dfrac{\partial\Psi_{0n}(x,y)}{\partial x}e^{j\omega t} \\ H_y(x,y,z) = -\dfrac{jk_z f(z)}{k_c^2}\dfrac{\partial\Psi_{0n}(x,y)}{\partial y}e^{j\omega t} \\ E_x(x,y,z) = -\dfrac{j\omega\mu f(z)}{k_c^2}\dfrac{\partial\Psi_{0n}(x,y)}{\partial y}e^{j\omega t} \\ E_y(x,y,z) = \dfrac{j\omega\mu f(z)}{k_c^2}\dfrac{\partial\Psi_{0n}(x,y)}{\partial x}e^{j\omega t} \\ E_z(x,y,z) = 0 \end{cases} , \quad (11)$$

where $f(z)$is the field profile function along the axis. Substituting Eq. 11 into Maxwell equations, the equation for the evolution of the EM wave amplitude in a confocal waveguide under the excitation of a current source can be obtained as:

$$\left(\frac{d^2}{dz^2} + k_z^2\right)f(z) = \frac{-2I_b}{N_{0n}} \times \sum_{j=0}^{N} W_j \frac{v_{\perp j}}{v_{zj}}\left[\cos\varphi\left(\frac{\partial\Psi_{0n}(x,y)}{\partial y}\right)^* - \sin\varphi\left(\frac{\partial\Psi_{0n}(x,y)}{\partial x}\right)^*\right]e^{-j\omega t} \quad , \quad (12)$$

where N is the total number of discrete electrons, and $v_{\perp j}$, $v_{zj}$are the transverse velocity and axis velocity of the electrons, respectively. In the beam-wave interaction of gyro-TWT, the electrons are mainly modulated by EM field and external static magnetic field. Therefore, the relativistic equation of motion is expressed as follows:

$$\frac{d\vec{p}}{dt} = -e\left[\vec{E} + \vec{v} \times \left(\vec{B}_{ext} + \vec{B}\right)\right] \quad , \quad (13)$$

where $\vec{p} = \gamma m_e \vec{v}$, $\vec{v}$ is the velocity, $\vec{E}$ and $\vec{B}$ are given by Eq. 11, and $\vec{B}_{ext}$ is the external field. Through the relation$\frac{d}{dz} = \frac{1}{v_z}\frac{d}{dt}$, and let $\vec{B}_1 = \vec{B}_{ext} + \vec{B}$, and after calculation and transformation, Eq. 13 that changes from the vector form to a series of scalar equations can be rewritten as follows:

$$\frac{d\beta_t}{dz} = -\frac{e}{\gamma m_e c^2 \beta_z}\left(1 - \beta_t^2\right)\left(E_x\cos\varphi + E_y\sin\varphi\right) - \frac{e}{\gamma m_e c}\left(B_{1x}\sin\varphi - B_{1y}\cos\varphi\right) \quad , \quad (14a)$$

$$\frac{\mathrm{d}\beta_z}{\mathrm{d}z}=\frac{e\beta_t}{\gamma m_e c^2}\left(E_x\cos\varphi+E_y\sin\varphi\right)+\frac{e\beta_t}{\gamma m_e c\beta_z}\left(B_{1x}\sin\varphi-B_{1y}\cos\varphi\right), \quad (14b)$$

$$\frac{\mathrm{d}\varphi}{\mathrm{d}z}=\frac{e}{\gamma m_e c^2\beta_t\beta_z}\left(E_x\sin\varphi-E_y\cos\varphi\right)-\frac{e}{\gamma m_e c\beta_t}\left(B_{1x}\cos\varphi+B_{1y}\sin\varphi\right)+\frac{e}{\gamma m_e c\beta_z}B_{1z}, \quad (14c)$$

$$\frac{\mathrm{d}r}{\mathrm{d}z}=\frac{\beta_t}{\beta_z}\cos\left(\varphi-\theta\right), \quad (14d)$$

$$\frac{\mathrm{d}\theta}{\mathrm{d}z}=\frac{\beta_t}{r\beta_z}\sin\left(\varphi-\theta\right), \quad (14e)$$

$$\frac{\mathrm{d}t}{\mathrm{d}z}=\frac{1}{c\beta_z}. \quad (14f)$$

All of the parameters are shown in Fig. 9. For a gyro-TWT, at the input end ($z=z_{in}$), the initial boundary condition is

$$f\left(z_{\mathrm{in}}\right)=\sqrt{\frac{2P_{\mathrm{in}}}{\omega\mu k_z N_{\mathrm{mn}}^2/k_c^2}}, \quad (15)$$

where P_{in} is the input power. Equations 10-15 constitute a set of frequency-domain steady-state, self-consistent nonlinear theory that can be applied to arbitrary cross section. A nonlinear numerical program was developed to analyze beam-wave interaction of confocal gyro-TWT.

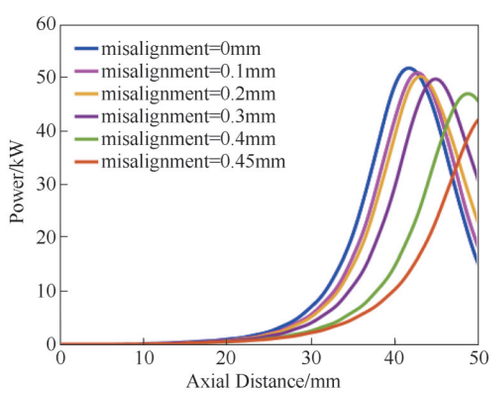

Fig. 10　Axial distributions of output power with electron beam misalignment
图 10　考虑电子注偏心时输出功率的轴向分布

By setting the input powerP_{in} as 30 W, the nonlinear theory derived previously can be applied to investigate the beam-wave interaction in presence of misaligned electron beam. Based on the nonlinear theory, the output power is calculated and analyzed in the situation of guiding center spread in a confocal waveguide gyro-TWT. As shown Fig. 10, it is obvious that the electron beam misalignment makes output power reduced at operating frequency. Meanwhile, the length of saturated power increases with the misalignment distance$d$, indicating that a longer interaction length is required to achieve the same power and gain. Meanwhile, the beam-wave efficiency and the length required for saturation versus electron beam misalignment distance are presented in

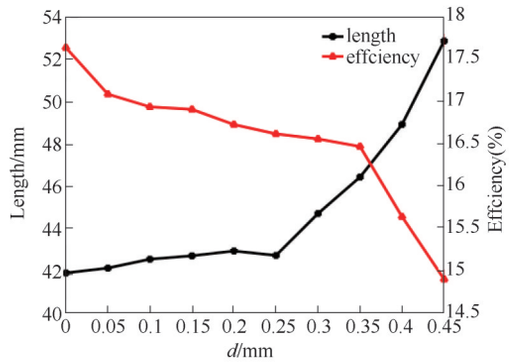

Fig. 11　The beam-wave efficiency and the saturation length versus misalignment distance d
图 11　注波互作用效率与饱和长度随偏心距离的变化

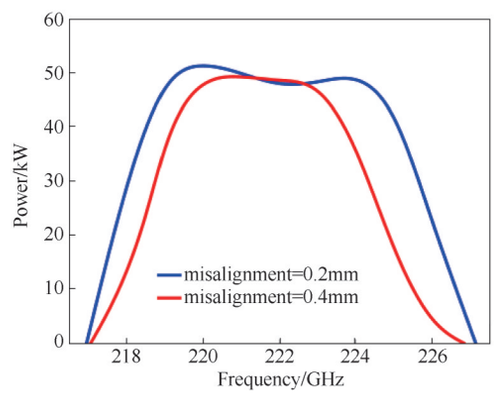

Fig. 12　Power versus frequency with electron beam misalignment
图 12　不同偏心时功率随频率的分布

Fig. 11. It is found that the saturation length is varied with the d when it changes from 0 to 0. 45 mm. In general, the saturation length increases with the increase of the misalignment distance, and the increase of length is more obvious for a larger value of misalignment distance$d$. At the same time, the efficiency decreases with the increase of the misalignment distance. Further, the reduction in efficiency causes a reduction in power. Figure 12 presents the curves of power with different electron beam misalignment$d$. It is clear that the power deviation is not too significant near the operating frequency but the bandwidth decreases considerably because of the decrease of efficiency.

The design parameters of the electron optical system will affect the quality of the electron beam, which is mainly manifested in the velocity spread and the guiding center spread of electron beam. Therefore, it is necessary to investigate the effect of electron beam quality on the beam-wave interaction. It can be seen from the Fig. 13 that as the velocity spread increases, the output power gradually decreases and the saturation length increases. Because the energy exchange of electrons that are in the same guiding center peak at different positions, which will affect the efficiency of interaction and the output power will take longer interaction length to its saturated state. Taking the velocity spread and electron

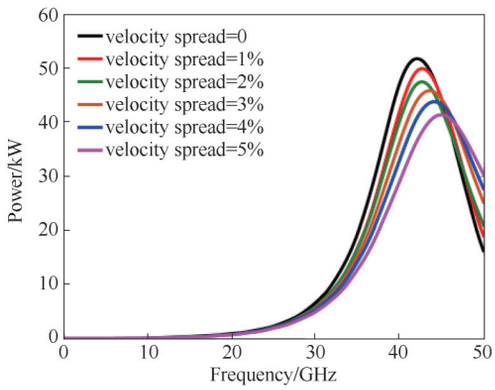

Fig. 13 Axial distributions of output power with velocity spread
图 13 考虑速度离散时输出功率的轴向分布

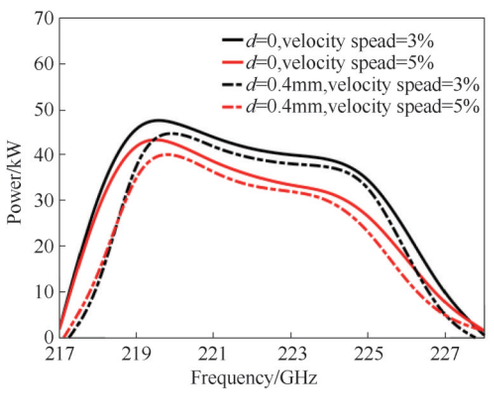

Fig. 14 Power versus frequency with velocity spread and guiding center spread
图 14 不同速度离散和偏心距离时的功率分布

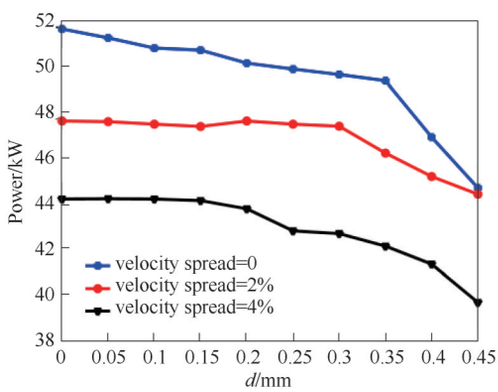

Fig. 15 The power versus the electron beam misalignment distance
图 15 功率随偏心距离的变化

beam misalignment into consideration, Fig. 14 illustrates relationship between the power and frequency. It is found that the variation trend of power is similar with the same value of misalignment distance*d*while the bandwidth decreases with increase of velocity spread. Meanwhile, the power decreases with the increase of velocity spread and misalignment distance. Figure 15 presents the variation of power versus the electron beam misalignment distance*d*. The power is varied with the increase of*d*. The power when the velocity spread is not taken into account is larger than that with velocity spread electron beam. Meanwhile, it is found that the variation of power is more notable for the electron beam without velocity spread especially when the misalignment distance is small. From Fig. 14-15, we can conclude that the quality of the electron beam, including velocity spread and guiding center spread, has a significant impact on the operation of the confocal gyro-TWT. It should be noted that we have only discussed the case where the electron beam is misaligned in the *x*-direction. However, due to the inhomogeneous field distribution of the confocal waveguide, the effect of the misaligned electron beam on the beam-wave interaction is more complicated when the electron beam is eccentric in the y-direction. In the future, we will pay more effort on the effect of misaligned electron beam in *y*-direction, which may be the topic of the next paper.

4 summery

The theoretical analysis methods of conventional gyrotron has been extended to confocal waveguide gyro-TWT and applied to case of electron beam misalignment. The effect of misaligned electron beam on the beam-wave interaction of a 0.22 THz confocal gyro-TWT has been investigated. Because of the special structure of confocal waveguide, the coupling factor varies considerably with the guiding centers of an annular electron beam, so the averaged coupling factor was applied to study the interaction between the asymmetric confocal mode and the annular electron beam with eccentricity. Based on the linear dispersion relationship, it is found that gain decreases with the increase of misalignment distance*d*. For instabilities, the value of critical current of TE_{06} mode absolute instability and the critical length of TE_{05} mode BWO are increased when the misalignment distance of electron beam increases. Moreover, the effect of misaligned electron beam on the efficiency is also investigated based on the self-consistent nonlinear theory of confocal gyro-TWT. The power and efficiency decrease with the increase of misalignment distance*d*. Further, the effect of velocity spread on the beam-wave interaction is also demonstrated in the nonlinear analysis. It is found that the velocity spread can deteriorate the efficiency of beam-wave interaction and the power decreases with the increasing velocity spread. All the above results indicate that the electron beam misalignment can have a significant impact on the performance of confocal gyro-TWT.

Acknowledgment

This work was supported by National Natural Science Foundation of China under contract 61571418, 61531002.

References

[1] Chu K R. Overview of research on the gyrotron traveling-wave amplifier [J]. *IEEE Trans. Plasma Sci*, 2002, **30**(3):903-908.
[2] Booske J H, Dobbs R J, Joye C D, *et al*. Vacuum electronic high power terahertz sources [J]. *IEEE Trans. Terahertz Science and Technology*, 2011, **1**(1):54-75.

[3] Glyavin M Y, Idehara T, Sabchevski S P. Development of THz gyrotrons at IAP RAS and FIR UF and their applications in physical research and high-power THz technologies [J]. *IEEE Transactions on Terahertz Science Technol*. 2015, **5**(5):788-797.
[4] Joye C D. A novel wideband 140 GHz gyrotron amplifier [D]. Ph.D. dissertation, Dept. Elect. Eng. Comput. Sci., Massachusetts Inst. Technol., Cambridge, MA, USA, 2008.
[5] Lau Y Y, Chu K R, Barmett L R, *et al*. Gyrotron traveling wave amplifier: I. Analysis of oscillation [J]. *Int. J. Infrared Millim. Waves*, 1981, **2**(3):373-395.
[6] Garven M, Calame J P, Danly B G, *et al*. A gyrotron-traveling-wave tube amplifier experiment with a ceramic loaded interaction region [J]. *IEEE Trans. Plasma Sci*, 2002, **30**(3):885-893.
[7] McDermott D B, Song S H, Hirata Y, *et al*. Design of a W-band TE01 mode gyrotron-traveling wave amplifier with high power and broad-band capabilities [J] *IEEE Trans. Plasma Sci*, **2002 30**(3): 894-902.
[8] Sirigiri J R, Shapiro M A, Temkin R J. High-power 140-GHz quasi-optical gyrotron traveling-wave amplifier [J]. *Phys. Rev. Lett*, 2003, **90**(25):258302.
[9] Yang Y, Yu S, Liu Y, *et al*. Efficiency enhancement of a 170 GHz confocal gyrotron traveling wave tube [J]. *Journal of Fusion Energy*, 2015, **34**(4):721-726.
[10] Hu W, Shapiro M, Michael A, *et al*. 140-GHz gyrotron experiments based on a confocal cavity [J]. *IEEE Trans. Plasma Sci*, 1998, **26** (3):366-374.
[11] Dumbrajs O, Nusinovich G S. Effect of electron beam misalignments on the gyrotron efficiency [J]. *Physics of Plasmas*, 2013, **20**(7): 073105.
[12] Dumbrajs O, Shenggang L. Kinetic theory of electron-cyclotron resonance masers with asymmetry of the electron beam in a cavity [J]. *IEEE Trans. Plasma Sci*, 1992, **20**(3):126-132.
[13] Nusinovich G S, Dumbrajs O, Levush B. Wave interaction in gyrotons with off-axis electron beams [J]. *Physics of Plasmas*, 1995, **2** (2):4621.
[14] Airila I M. Degradation of operation mode purity in a gyrotron with an off-axis electron beam [J]. *Physics of Plasmas*, 2003, **10** (1): 296-299.
[15] Sun W, Yu S, Wang Z, *et al*. Linear and nonlinear analyses of a 0.34-THz confocal waveguide gyro-TWT [J] *IEEE Trans. Plasma Sci*. 2018, **46**(3):511-517.
[16] Hu W. Studies of novel 140 GHz gyrotrons [D]. Ph.D. dissertation, Dept. Phys., Massachusetts Inst. Technol., Cambridge, MA, USA, 1997
[17] Soane A V, Shapiro M A, Stephens J C, *et al*. Theory of linear and nonlinear gain in a gyroamplifier using a confocal waveguide [J] *IEEE Trans. Plasma Sci*, 2017, **45**(9):2438-2449.
[18] Chu K R, Lin A T. Gain and bandwidth of the gyro-TWT and CARM amplifiers [J], *IEEE Trans. Plasma Sci*, 1988, **16**(2):90-104
[19] Sangster A J. Small-signal analysis of the travelling-wave gyrotron using pierce parameters [J]. *Communications, Speech and Vision, IEE Proceedings I*, 1980, **127**(2):45-52
[20] Davies, John A. Conditions for absolute instability in the cyclotron resonance maser [J]. *Physics of Fluids B Plasma Physics*, 1989, **1** (3):663-669.